

Multimodal Image-to-Image Translation via Mutual Information Estimation and Maximization

Zhiwen Zuo¹ Lei Zhao¹ Zhizhong Wang¹ Haibo Chen¹ Ailin Li¹ Qijiang Xu²
 Wei Xing¹ Dongming Lu¹

¹ Zhejiang University ² Kwai Inc.

{zzwcs, cszhl, endywon, feng123, liailin, wxing, ldm}@zju.edu.cn, xuqijiang@kuaishou.com

Abstract

Multimodal image-to-image translation (I2IT) aims to learn a conditional distribution that explores multiple possible images in the target domain given an input image in the source domain. Conditional generative adversarial networks (cGANs) are often adopted for modeling such a conditional distribution. However, cGANs are prone to ignore the latent code and learn a unimodal distribution in conditional image synthesis, which is also known as the mode collapse issue of GANs. To solve the problem, we propose a simple yet effective method that explicitly estimates and maximizes the mutual information between the latent code and the output image in cGANs by using a deep mutual information neural estimator in this paper. Maximizing the mutual information strengthens the statistical dependency between the latent code and the output image, which prevents the generator from ignoring the latent code and encourages cGANs to fully utilize the latent code for synthesizing diverse results. Our method not only provides a new perspective from information theory to improve diversity for I2IT but also achieves disentanglement between the source domain content and the target domain style for free. Extensive experiments under both paired and unpaired I2IT settings demonstrate the effectiveness of our method to achieve diverse results without loss of quality. Our code will be made publicly available soon.

1. Introduction

In recent years, Generative Adversarial Networks (GANs) [20] have emerged as a promising generative model that can capture complex and high-dimensional image data distributions. Extended on GANs, conditional GANs (cGANs) [41] which take extra contextual information as input are widely applied in conditional image synthesis tasks and achieve great success, such as image to image translation [25], super resolution [32], image inpaint-

ing [47], and text-to-image synthesis [60].

Domain mapping or image-to-image translation (I2IT) aims to learn the mapping from the source image domain \mathcal{A} to the target image domain \mathcal{B} . Many conditional image synthesis tasks can be seen as special cases of I2IT, e.g., super resolution [32], colorization [31], image inpainting [47], and style transfer [18]. However, many previous works [25, 54, 37, 64] on I2IT only learn a deterministic mapping function. I2IT should be capable of producing multiple possible outputs even for a single input image, e.g., a Yosemite winter photo may correspond to multiple summer photos that vary in light, the amount of clouds, or the luxuriance of vegetation. A straightforward way to produce diverse results for cGANs is to distill such variations in latent noise Z that can be sampled from a simple distribution, such as an isotropic Gaussian. However, this problem is inherently ill-posed as there are usually only one or even no corresponding images available in the target domain for an input image in the source domain during training. And the signal from high-dimensional and structured input image is usually stronger than that of the low-dimensional latent noise in cGANs. It has been reported in the literature of conditional image synthesis [25, 38, 40, 65] that cGANs are prone to overlook the latent noise, which is also known as the mode collapse issue [19, 20, 50] of GANs.

To encourage diversity for I2IT, many existing works [1, 24, 33, 63, 65] propose to learn a *one-to-one mapping* between the latent space and the generated image space by using informative encoders to recover the latent code from the generated image, which we refer to as the *latent code reconstruction loss* in this paper. From a perspective of information theory, we show that this loss is highly related to the variational mutual information maximization [3, 9] between the latent code Z and the output image \hat{B} as follows (refer to supplementary materials for detailed derivation):

$$\mathcal{I}(Z; \hat{B}) = H(Z) - H(Z|\hat{B}) \geq H(Z) - \mathcal{L}_R \quad (1)$$

where $\mathcal{I}(\cdot; \cdot)$, $H(\cdot)$, and \mathcal{L}_R are the mutual information, the

Shannon entropy and the latent code reconstruction loss, respectively. As the entropy $H(Z)$ is a constant (the prior distribution p_z is often predefined), minimizing the latent code reconstruction loss \mathcal{L}_R amounts to maximizing a variational lower bound on the mutual information between Z and \hat{B} . Maximizing the mutual information improves diversity for cGANs as it enhances the statistical dependency between Z and \hat{B} and prevents the generator from ignoring Z . However, the latent code reconstruction loss is limited by the design of the specific task [24, 63, 65] and the capacity of the encoders to learn useful information [25, 30]. To bypass such restrictions and fully encourage the statistical dependency between the latent code Z and the output image \hat{B} , in this paper, we propose an alternative and straightforward way - discarding the encoders and directly maximizing the mutual information between them. This is achieved by the deep mutual information neural estimator [4]. Specifically, our method introduces a statistics network T to estimate and maximize the mutual information between the latent code Z and the output image $\hat{B} = G(\cdot, Z)$ by discriminating the corresponding positive samples $(z_1, G(\cdot, z_1))$ from the non-corresponding negative samples $(z_1, G(\cdot, z_2))$, as shown in Figure 1. Intuitively, this implies the statistics network tries to discover the unique link between the latent code and the images generated by it, which also indirectly decouples the target domain style from the source domain content.

We augment existing paired or unpaired I2IT methods with our proposed additional loss term that maximizes the mutual information between the latent code and the generated image to encourage diversity for them, e.g., pix2pix [25] and GcGAN [17]. A simple architectural enhancement is shown to suffice for the utilization of our proposed loss, which results in an elegant new model we name as Statistics Enhanced GAN (SEGAN) in this paper (see Figure 2). Both qualitative and quantitative evaluations under paired and unpaired I2IT settings verify the effectiveness of our method for improving diversity without loss of image quality.

Our contributions in this paper are summarized below:

- We propose a novel method from information theory that explicitly estimates and maximizes the mutual information between the latent code and the output image to palliate mode collapse in cGANs.
- Our method also achieves disentanglement between the source domain content and the target domain style for free.
- The proposed method can facilitate many existing I2IT methods to improve diversity with a simple network extension.
- Extensive experiments show the effectiveness of our method to improve diversity without sacrificing image

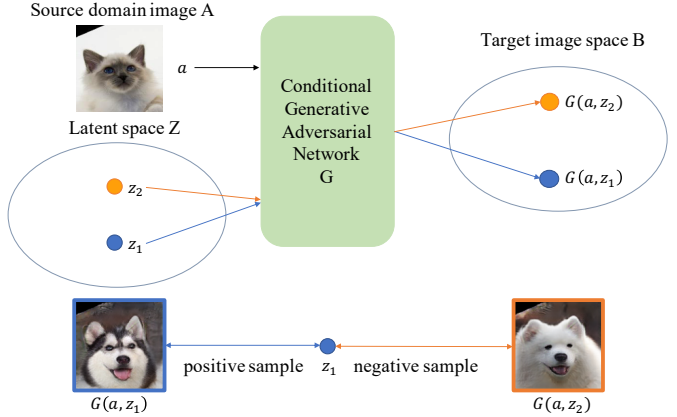


Figure 1. **Proposed method.** Our method encourages diversity for image-to-image translation by estimating and maximizing the deep neural mutual information between the latent code and the generated image in cGANs. Specifically, we classify the latent code and the images generated by it (e.g., $(z_1, G(a, z_1))$) and the latent code and the images not generated by it (e.g., $(z_1, G(a, z_2))$) as the positive and negative samples respectively.

quality of generated samples.

2. Related Works

2.1. Generative adversarial networks

Generative Adversarial Networks (GANs) [20] compose of two modules: a discriminator that tries to distinguish real data samples from generated samples, and a generator that tries to generate samples to fool the discriminator. Many important works are proposed to improve the original GAN for more stabilized training and producing high-quality samples, such as by proposing better loss functions or regularizations [2, 21, 7, 39, 42, 62], changing network structures [13, 26, 27, 48, 59], or combining inference networks or autoencoders [8, 14, 16, 30, 51, 53]. In this work, we rely on GANs to synthesize realistic and diverse images for multimodal image-to-image translation.

2.2. Multimodal image-to-image translation

We classify the current multimodal image-to-image translation (I2IT) methods into three categories according to the techniques encouraging diversity for them: (1) latent code reconstruction loss, including AugCycleGAN [1], BicycleGAN [65], MUNIT [24], DRIT [33], SDIT [55], and DMIT [58], (2) simply maximizing the pixel difference between the generated images, including MS-GAN [38] and DSGAN [56], and (3) the combination of both the above two techniques, including StarGANv2 [10] and DRIT++ [34]. Specifically, SDIT [55], DMIT [58], DRIT++ [34], and StarGANv2 [10] combine the multimodal and the multidomain I2IT in a unified model by uti-

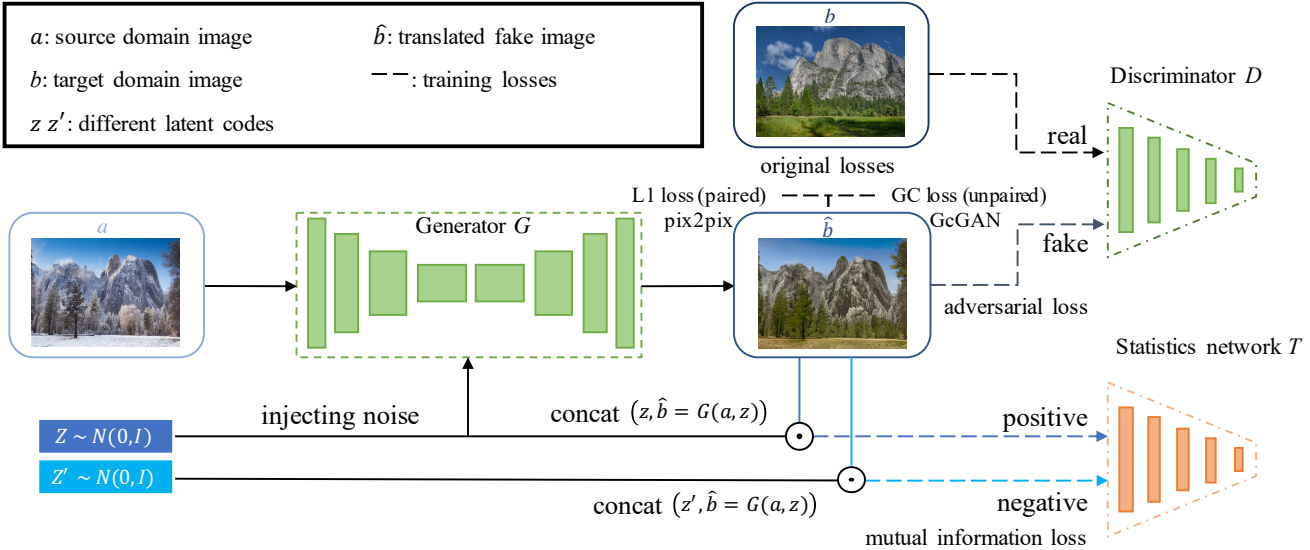


Figure 2. The network architecture and training losses of SEGAN. Our model contains two modules: a conditional generative adversarial network (with a generator G and a discriminator D) and a statistics network T . We build our method on pix2pix [25] and GcGAN [17] under paired and unpaired settings respectively. The mutual information between the latent code and the output image is maximized by discriminating the corresponding positive samples from the non-corresponding negative samples.

lizing a domain label. However, these methods still rely on the techniques mentioned above to encourage diverse results. In later experiments, we will compare our method with BicycleGAN [65] and MSGAN [38] under a paired setting, and MUNIT [24], DRIT [33], and DRIT++ [34] under an unpaired setting, to demonstrate the effectiveness and superiority of our proposed method.

2.3. Mutual information

Mutual Information (MI) is a fundamental quantity for measuring the relationship between random variables. In contrast to correlation, mutual information can capture non-linear statistical dependencies between variables, and thus can act as a measure of true dependence [29]. Methods based on Mutual Information (MI) can date back to the infomax principle [5, 36], which advocates maximizing MI between the input and the output of the neural networks. Notably, InfoGAN [9] proposed to maximize the MI between a small part of the latent code and the generated outputs in GANs for discovering disentangled latent representations. Our method, though shares a similar idea with InfoGAN about maximizing the MI, yet differs from InfoGAN in two main aspects. First, in methodology, InfoGAN minimizes a variational lower bound on the conditional entropy and ignores the sample entropy of the MI (refer to supplementary materials), while our method explicitly estimates and maximizes the whole MI term. Second, in target, InfoGAN aims to disentangle latent factors in GANs, while our method mainly attacks the mode collapse issue in cGANs. On the other hand, in BicycleGAN [65], the authors at-

tempted to use cLRGAN which is a conditional version of InfoGAN to encourage diversity for paired I2IT, but it resulted in less variation in the output and sometimes failed in severe mode collapse, probably because the simple latent code reconstruction loss does not fulfill the maximization of the MI in conditional image synthesis. In contrast, we show that our proposed method can successfully maximize the MI and therefore improves diversity for I2IT.

Some neural estimators of MI have been proposed in recent years, such as MINE [4] and InfoNCE [45]. Intuitively, these methods estimate MI between random variables X and Y by training a classifier to distinguish between the corresponding samples drawn from the joint distribution $p(x, y)$ and the non-corresponding samples drawn from the product of marginals $p(x)p(y)$. ALICE [35] revealed that cycle consistency [28, 64, 57] is actually maximizing a lower bound on the MI between the input and the output of the generator. Based on that, CUT [46] adopts the InfoNCE loss to maximize the MI between the corresponding patches of the input and the output to preserve content information for unpaired I2IT recently. However, our target and methodology are totally different from CUT: (1) The target of CUT is to better preserve the content for unpaired I2IT, which *can only produce unimodal results*. Our method aims to *yield diverse results* for I2IT and theoretically can be combined with CUT to encourage diversity for it. (2) The methodology is also different. CUT uses *NCE loss* to maximize MI between *the corresponding patches of the input and the output images*, which cannot be used in our case. We formulate a *JSD MI estimator* to estimate and

maximize the MI between *the latent code and the output image*. The mathematical form of our loss is a binary cross-entropy, which does not require a large negative sample size per positive sample as in NCE loss; thus, it is more stable and easier to implement.

3. Statistics Enhanced GAN

3.1. Preliminaries

Suppose we have a source image domain $\mathcal{A} \subset \mathbb{R}^{H \times W \times 3}$ and a target image domain $\mathcal{B} \subset \mathbb{R}^{H \times W \times 3}$, multimodal image-to-image translation (I2IT) refers to learning a generator’s function $G(a, z)$ such that $a \in \mathcal{A}$, $\hat{b} = G(a, z) \in \mathcal{B}$ and \hat{b} preserves some underlying spatial information of a ¹. We refer to such underlying spatial information and the semantic difference of the target image domain as “content” and “style” respectively. An adversarial loss shown below is used to ensure $G(a, z)$ to look like real samples from the target image domain. And the latent code Z is responsible for the style variations of the output image \hat{b} .

$$\max_{D_\theta} \min_{G_\gamma} \mathbb{E}_{b \sim p(b)} [\log D_\theta(b)] + \mathbb{E}_{a \sim p(a), z \sim p(z)} [\log(1 - D_\theta(G_\gamma(a, z)))] \quad (2)$$

where D , $D(\cdot)$, θ , G , $G(\cdot, \cdot)$, and γ are the discriminator, the discriminator’s critic function, the parameters of the discriminator, the generator, the generator’s function, and the parameters of the generator, respectively.

For simplicity, Z often follows a standard Gaussian such that $z \sim \mathcal{N}(0, I)$. After training, we expect that varying the latent noise conditioned on an input image can produce different images varying in style while preserving the content. However, several previous works [25, 38, 40, 65] have reported that naively adding the noise can hardly produce diverse results, probably because of the mode collapse issue of GANs.

3.2. Probabilistic analysis

To encourage diversity for image-to-image translation (I2IT), we propose to enhance the connection between the latent noise Z and the output image \hat{B} in a statistical manner by maximizing the mutual information between them, therefore we call our proposed model Statistics Enhanced GAN (SEGAN).

Why maximizing the MI between Z and \hat{B} helps to reduce mode collapse in cGANs? Suppose the latent noise Z is ignored by the generator which is often encountered in conditional image synthesis tasks [25, 38, 40, 65], the generator’s function $G(a, z)$ and the conditional distribution $p(\hat{b}|a, z)$ modeled by cGANs would degenerate to $G(a)$

¹We use uppercase letters for random variables and lowercase letters for realizations of these random variables.

and $p(\hat{b}|a)$ respectively, which means Z is independent of \hat{B} and the translation becomes deterministic. In information theory, such dependency is measured by the Mutual Information (MI). The MI between the latent code Z and the output image \hat{B}

$$\mathcal{I}(\hat{B}; Z) = H(\hat{B}) - H(\hat{B}|Z) = H(Z) - H(Z|\hat{B}) \quad (3)$$

quantifies the “amount of information” of \hat{B} through observing Z . When the generator overlooks Z (which means Z is independent of \hat{B}), the MI attains its minimal value $\mathbf{0}$, because knowing Z reveals nothing about \hat{B} under such circumstances. In contrast, if Z and \hat{B} are closely related by an invertible function, *e.g.*, Z is utilized by the generator to represent different styles of the target image domain, then the MI attains its maximum. From another perspective, the direct way to encourage diversity of a random variable is to maximize its entropy. As the generated sample’s entropy $H(\hat{B})$ is intractable, we use the MI between \hat{B} and Z as a proxy. As shown in Equation 3, the MI can be seen as a lower bound on $H(\hat{B})$.

3.3. Architecture and disentanglement

SEGAN is simple and neat in its architecture: it is merely an extension upon cGANs with a statistics network T as shown in Figure 2. The statistics network is used to estimate and maximize the Mutual Information (MI) between the latent noise Z and the output image \hat{B} .

In our method, the statistics network T estimates and maximizes the MI by performing a binary classification between the “positive samples” ($z, G(\cdot, z)$) (the latent code and the images generated by it) and the “negative samples” ($z', G(\cdot, z')$) (the latent code and the images not generated by it). This indicates the statistics network has to find out the universal influence that the latent code z puts on the output image $G(a, z)$ regardless of the input image a (because a fixed z can be combined with many different source domain images a). As such, the method forces the latent code to represent the style of the target image domain instead of the noises or the structures of the content. Once successfully trained, our method therefore achieves disentanglement between the source domain content and the target domain style for free.

3.4. Loss functions

Mutual information loss. Formally, the Mutual Information (MI) between random variables X and Y is defined as the Kullback-Leibler (KL) divergence between the joint distribution $p(x, y)$ and the product of the marginals $p(x)p(y)$:

$$\begin{aligned} \mathcal{I}(X; Y) &= D_{\text{KL}} [p(x, y) \| p(x)p(y)] \\ &= \mathbb{E}_{p(x, y)} \left[\log \frac{p(x, y)}{p(x)p(y)} \right] \end{aligned} \quad (4)$$

Belghazi *et al.* [4] propose several neural estimators of MI based on the dual formulations of the KL-divergence, that are trainable through back-propagation and highly consistent, such as the Donsker-Varadhan (DV) representation [15] and the f-divergence representation [43, 44]. However, these estimators have some defeats making them difficult to be applied for practical use, such as biased estimate of the batch gradient and unbounded value [4]. For a more stabilized training, we adopt a neural estimator that lower bounds the Jensen-Shannon Divergence (JSD) between the joint and the product of the marginals following the formulation of f-GAN [44]. This JSD MI estimator is more stable and positively correlated with MI (refer to supplementary materials for the proof):

$$\begin{aligned} \text{JSD} [p(z, \hat{b}) \| p(z)p(\hat{b})] &\geq \\ \hat{\mathcal{I}}_{\omega}^{\text{JSD}}(Z; G_{\gamma}(\cdot, Z)) &= \mathbb{E}_{p_z} [\log(\sigma(T_{\omega}(z, G_{\gamma}(\cdot, z))))] + \\ \mathbb{E}_{\hat{p}_z \times p_z} [\log(1 - \sigma(T_{\omega}(z', G_{\gamma}(\cdot, z))))] & \end{aligned} \quad (5)$$

where $\hat{b} = G_{\gamma}(\cdot, z)$, $T_{\omega}(\cdot, \cdot)$ is the statistics network’s function with parameters ω that outputs a scalar, $p_z = \hat{p}_z = \mathcal{N}(0, I)$, z and z' are different samples from $\mathcal{N}(0, I)$, and $\sigma(\cdot)$ is the sigmoid function. The mathematical form of the JSD MI estimator amounts to the familiar binary cross-entropy. The MI is estimated by maximizing $\hat{\mathcal{I}}_{\omega}^{\text{JSD}}$ in Equation 5 w.r.t. the statistics network’s parameters ω .

As maximizing MI follows the same direction of estimating MI, we jointly optimize the generator and the statistics network by the mutual information loss below:

$$\mathcal{L}_{\text{MI}} = \max_{T_{\omega}, G_{\gamma}} \hat{\mathcal{I}}_{\omega}^{\text{JSD}}(Z; G_{\gamma}(\cdot, Z)) \quad (6)$$

Total loss. Our method can be combined with any existing I2IT methods to improve diversity for them as long as they are built on cGANs. Thus, the final loss function for training can be formulated by adding our proposed mutual information loss to the original losses of the existing method:

$$\mathcal{L}_{\text{total}} = \mathcal{L}_{\text{ori}} + \lambda_{\text{MI}} \mathcal{L}_{\text{MI}} \quad (7)$$

where \mathcal{L}_{ori} is the original losses and λ_{MI} is the weight that controls the importance of our mutual information loss.

4. Experiments

4.1. Baselines and compared methods

We evaluate our method by building it on pix2pix [25] and GcGAN [17] under paired and unpaired settings respectively. Therefore, the baselines are naively adding noise to pix2pix and GcGAN and we call them as SEGAN w/o MI. Under a paired setting, we also compare our method

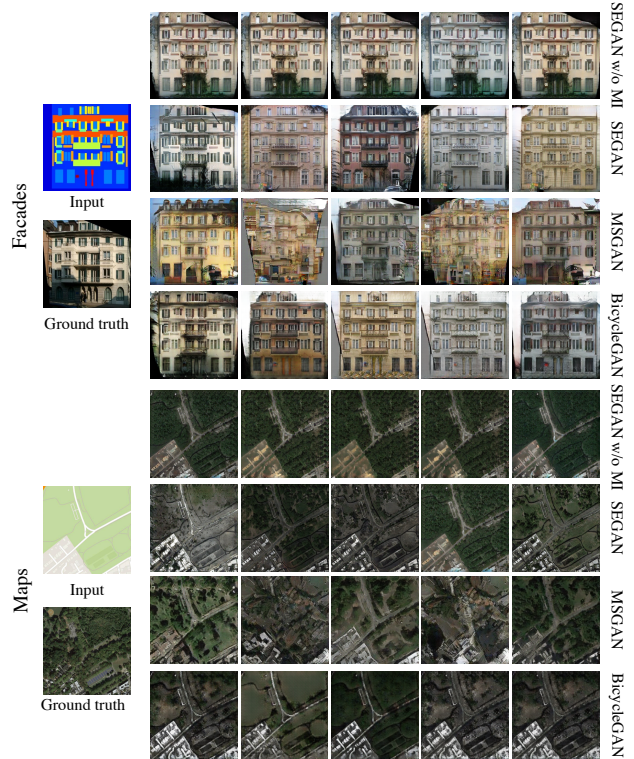


Figure 3. Qualitative results of different methods on the Facades and Maps datasets under a paired setting.

(SEGAN) with two of the state-of-the-art methods: BicycleGAN [65] and MSGAN [38]. Under an unpaired setting, we compare ours with some state-of-the-art multimodal unsupervised I2IT methods, *e.g.*, MUNIT [24], DRIT [33], and DRIT++ [34].

4.2. Datasets

Under a paired setting, we evaluate on Google maps→satellite (Maps) [25] and labels→images (Facades) [11]. Under an unpaired setting, we perform experiments on a shape-invariant dataset: Yosemite winter→summer [64] and a shape-variant dataset: cat→dog [33].

4.3. Metrics

For quantitative evaluation, we mainly use four metrics: FID [22], NDB [49], JSD [49], and LPIPS [61].

FID. FID measures the quality of generated images by calculating the distance between the model distribution and the real one through deep features extracted by Inception network [52]. Lower FID values indicate higher quality.

NDB and JSD. NDB and JSD [49] are two bin-based metrics. The training data is first clustered by K-means into different bins which can be viewed as modes of the real data

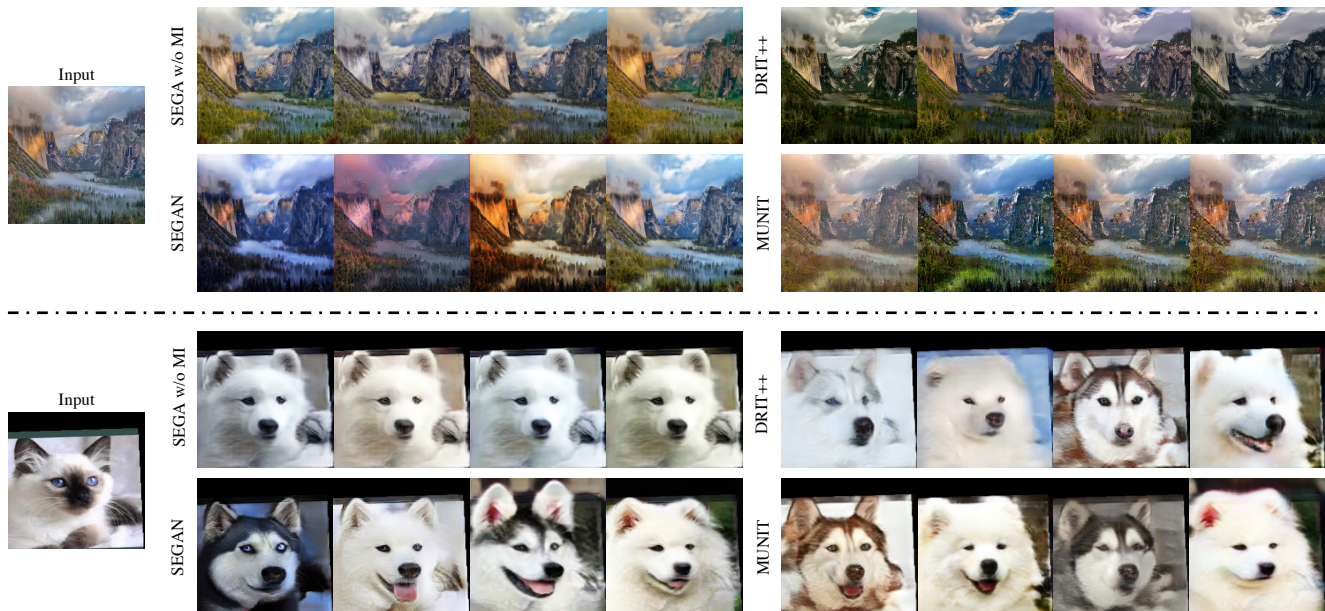


Figure 4. Qualitative results of different methods on the Yosemite winter→summer and cat→dog datasets under an unpaired setting.

distribution. Then each generated sample is assigned to the bin of its nearest neighbor. Two-sample test is performed on each bin and then the number of statistically-different bins (NDB) is reported. The Jensen-Shannon Divergence (JSD) between the training data’s bins distribution and the generated data’s bins distribution is also reported. For both two metrics, lower values indicate higher diversity.

LPIPS. LPIPS [61] measures the averaged feature distances between generated samples conditioned on the same input image. Higher LPIPS score indicates better diversity among the generated images.

4.4. Implementation details

We adopt the original non-saturation GAN loss [20] for training. As our proposed neural estimator needs a relatively large batch size to stabilize the training and reduce variance in estimation, we use a batch size of 32 in our experiments. After a hyperparameter search on λ_{MI} in preliminary experiments, we find setting it as 3 is the best and consistently set $\lambda_{MI} = 3$ in all our experiments. The statistics network is a Convolutional Neural Network (CNN) followed by a few fully-connected layers. The choice of sampling strategy is important to make our algorithm work. As suggested in [23], we exclude the positive samples from the product of marginals. For more details, please refer to the supplementary materials.

4.5. Mutual information maximization

Figure 5 shows the change of the estimate of MI by our JSD MI estimator during training on the Facades dataset.

In the beginning, as Z does not play a role in producing diverse results, the statistics network can not tell the positive samples apart from the negative samples, and thus it makes a random guess on them, resulting in a quantity of $\log 0.5 + \log 0.5 \approx -1.386$ (see Equation 5). And as the training proceeds, the estimate of the MI is maximized to 0, which means the statistics network can faithfully discriminate the positive samples from negative samples.

4.6. Paired image-to-image translation

We build our method on pix2pix [25] under a paired I2IT setting. For a fair comparison, all methods use the same network architecture as in BicycleGAN [65]. We set the weight of L1 loss as 3 in our method. SEGAN consistently improves on all metrics over the baseline method as shown in Table 1. Note that SEGAN w/o MI has better FIDs than BicycleGAN and MSGAN [38], probably due to the relatively large batch size we used. We also tried using the same batch size for training BicycleGAN and MSGAN but obtained no performance gains. Compared with the state-of-the-art methods, our method’s diversity outper-

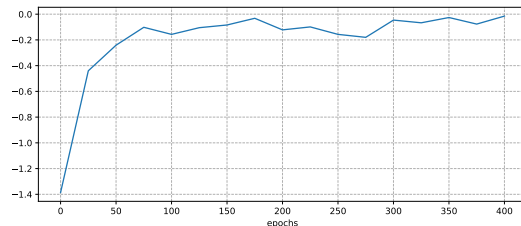


Figure 5. The change of the estimate of MI by our JSD MI estimator during training on Facades dataset.

Dataset	Facades			
	SEGAN w/o MI	SEGAN	BicycleGAN [65]	MSGAN [38]
FID ↓	89.14 ± 0.99	78.43 ± 1.15	98.85 ± 1.21	92.84 ± 1.00
NDB ↓	14.40 ± 0.65	11.60 ± 0.80	13.80 ± 0.45	12.40 ± 0.55
JSD ↓	0.068 ± 0.003	0.036 ± 0.005	0.058 ± 0.004	0.038 ± 0.0011
LPIPS ↑	0.1038 ± 0.0015	0.1897 ± 0.0015	0.1413 ± 0.0005	0.1894 ± 0.0011
Dataset	Maps			
	SEGAN w/o MI	SEGAN	BicycleGAN [65]	MSGAN [38]
FID ↓	126.73 ± 1.47	119.51 ± 0.62	145.78 ± 3.90	152.46 ± 2.52
NDB ↓	47.40 ± 1.50	40.72 ± 1.00	46.60 ± 1.34	41.60 ± 0.55
JSD ↓	0.048 ± 0.002	0.021 ± 0.002	0.023 ± 0.002	0.031 ± 0.003
LPIPS ↑	0.1121 ± 0.002	0.1972 ± 0.003	0.1142 ± 0.001	0.2049 ± 0.002

Table 1. Quantitative results of different methods on the Facades and the Maps datasets under a paired setting.

Dataset	Winter → Summer				
	SEGAN w/o MI	SEGAN	MUNIT [24]	DRIT [33]	DRIT++ [34]
FID ↓	50.05 ± 0.64	40.72 ± 0.82	57.09 ± 0.37	41.34 ± 0.20	41.02 ± 0.24
NDB ↓	10.33 ± 0.85	9.15 ± 0.67	9.53 ± 0.64	9.38 ± 0.74	9.22 ± 0.97
JSD ↓	0.302 ± 0.052	0.210 ± 0.070	0.293 ± 0.062	0.304 ± 0.075	0.222 ± 0.070
LPIPS ↑	0.1032 ± 0.0007	0.1381 ± 0.0004	0.1136 ± 0.0008	0.0965 ± 0.0004	0.1183 ± 0.0007
Dataset	Cat → Dog				
	SEGAN w/o MI	SEGAN	MUNIT [24]	DRIT [33]	DRIT++ [34]
FID ↓	28.86 ± 0.35	17.20 ± 0.22	22.13 ± 0.71	24.31 ± 0.33	17.25 ± 0.65
NDB ↓	9.70 ± 0.51	7.52 ± 1.35	8.21 ± 1.17	8.16 ± 1.60	7.57 ± 1.25
JSD ↓	0.144 ± 0.030	0.037 ± 0.023	0.132 ± 0.066	0.075 ± 0.046	0.041 ± 0.014
LPIPS ↑	0.231 ± 0.002	0.282 ± 0.002	0.244 ± 0.002	0.245 ± 0.002	0.280 ± 0.002

Table 2. Quantitative results of the Yosemite winter→summer and the cat→dog datasets under an unpaired setting.

forms BicycleGAN and is comparable to MSGAN (as measured by NDB, JSD, and LPIPS) while with a higher quality (as measured by FID). We can also observe that MSGAN sometimes produces images with artifacts and distortions as shown in Figure 3, which may be caused by the objective function of MSGAN that simply maximizes the pixel difference between output images. More qualitative results can be found in supplementary materials.

4.7. Unpaired image-to-image translation

Under an unpaired setting, we choose a one-sided unpaired I2IT method GcGAN [17] as the baseline (theoretically our method can also be combined with DistanceGAN [6] or CUT [46]), resulting in a much simpler and fast-training framework compared with methods like MUNIT [24], DRIT [33], and DRIT++ [34] (see Figure 2). For simplicity, we use a U-net generator and a multi-scale discriminator as in BicycleGAN [65]. The U-net generator can also help preserve the content as its skip-connections propagate the shape information directly from input to output. We

set the weight of geometry-consistency (GC) loss as 20. We find that GC loss is useful for shape-invariant datasets like Yosemite winter→summer, but may degrade the quality for shape-variant datasets like cat→dog. So we omit it when trained on cat→dog and find that the U-net generator architecture is sufficient for preserving the input image’s pose.

Figure 4 and Table 2 show different methods’ qualitative and quantitative results on Yosemite winter→summer and cat→dog datasets. Our method surpasses the baseline method on diversity without loss of quality. While with a much simpler network architecture and a smaller training budget than the state-of-the-art methods, *e.g.*, MUNIT and DRIT++, our method also beat them with a noticeable margin, verifying the robustness of our method to improve diversity without loss of quality for I2IT.

Our method can also achieve disentanglement between the source domain content and the target domain style for free. We produce synchronized results using the same code for each style on the Yosemite winter→summer dataset. In Figure 6, it can be seen that each latent code represents a



Figure 6. Disentangled results of our method on the Yosemite winter→summer dataset under an unpaired setting. Each column’s images are produced by the same latent code.



Figure 7. Translated samples generated from linear-interpolated vectors between two latent code vectors.

uniform style regardless of the input image. In addition, we perform linear interpolation between two given latent codes to show the generalization of our method to capture the conditional distribution. In Figure 7, the interpolation reflects smooth changes in semantic level, *e.g.*, the daylight and the tongue patten changes gradually with the variations of the latent codes. More qualitative results can be found in supplementary materials.

5. Conclusions and discussions

We have presented a novel method to encourage diversity for image-to-image translation by adopting a deep neural estimator to estimate and maximize the mutual information

between the latent code and the generated image in cGANs. A simple network enhancement to cGANs is proved to be sufficient for using our proposed loss. Our method can also disentangle target domain style from the source domain content for free. Extensive qualitative and quantitative evaluations demonstrate the effectiveness of our method to improve diversity without loss of quality.

Furthermore, we would like to discuss the wide application domains that may benefit from our method, *e.g.*, other conditional image synthesis tasks that desire diversity (like image inpainting, text-to-image synthesis, and style transfer), disentangling latent factors in a conditional generative model setting, and encouraging diversity in conditional image generation (like on ImageNet [12]).

References

- [1] Amjad Almahairi, Sai Rajeswar, Alessandro Sordani, Philip Bachman, and Aaron Courville. Augmented cyclegan: Learning many-to-many mappings from unpaired data. *arXiv preprint arXiv:1802.10151*, 2018. [1](#), [2](#)
- [2] Martin Arjovsky, Soumith Chintala, and Léon Bottou. Wasserstein gan. *arXiv preprint arXiv:1701.07875*, 2017. [2](#)
- [3] David Barber and Felix V Agakov. The im algorithm: a variational approach to information maximization. In *Advances in neural information processing systems*, page None, 2003. [1](#), [12](#)
- [4] Mohamed Ishmael Belghazi, Aristide Baratin, Sai Rajeswar, Sherjil Ozair, Yoshua Bengio, Aaron Courville, and R Devon Hjelm. Mine: mutual information neural estimation. *arXiv preprint arXiv:1801.04062*, 2018. [2](#), [3](#), [5](#)
- [5] Anthony J Bell and Terrence J Sejnowski. An information-maximization approach to blind separation and blind deconvolution. *Neural computation*, 7(6):1129–1159, 1995. [3](#)
- [6] Sagie Benaim and Lior Wolf. One-sided unsupervised domain mapping. In *Advances in neural information processing systems*, pages 752–762, 2017. [7](#)
- [7] David Berthelot, Thomas Schumm, and Luke Metz. Began: Boundary equilibrium generative adversarial networks. *arXiv preprint arXiv:1703.10717*, 2017. [2](#)
- [8] Tong Che, Yanran Li, Athul Paul Jacob, Yoshua Bengio, and Wenjie Li. Mode regularized generative adversarial networks. *arXiv preprint arXiv:1612.02136*, 2016. [2](#)
- [9] Xi Chen, Yan Duan, Rein Houthoofd, John Schulman, Ilya Sutskever, and Pieter Abbeel. Infogan: Interpretable representation learning by information maximizing generative adversarial nets. In *Advances in neural information processing systems*, pages 2172–2180, 2016. [1](#), [3](#), [12](#)
- [10] Yunjey Choi, Youngjung Uh, Jaejun Yoo, and Jung-Woo Ha. Stargan v2: Diverse image synthesis for multiple domains. In *Proceedings of the IEEE/CVF Conference on Computer Vision and Pattern Recognition*, pages 8188–8197, 2020. [2](#)
- [11] Marius Cordts, Mohamed Omran, Sebastian Ramos, Timo Rehfeld, Markus Enzweiler, Rodrigo Benenson, Uwe Franke, Stefan Roth, and Bernt Schiele. The cityscapes dataset for semantic urban scene understanding. In *Proceedings of the IEEE conference on computer vision and pattern recognition*, pages 3213–3223, 2016. [5](#)
- [12] Jia Deng, Wei Dong, Richard Socher, Li-Jia Li, Kai Li, and Li Fei-Fei. Imagenet: A large-scale hierarchical image database. In *2009 IEEE conference on computer vision and pattern recognition*, pages 248–255. Ieee, 2009. [8](#)
- [13] Emily Denton, Soumith Chintala, Arthur Szlam, and Rob Fergus. Deep generative image models using a laplacian pyramid of adversarial networks. *arXiv preprint arXiv:1506.05751*, 2015. [2](#)
- [14] Jeff Donahue, Philipp Krähenbühl, and Trevor Darrell. Adversarial feature learning. *arXiv preprint arXiv:1605.09782*, 2016. [2](#)
- [15] Monroe D Donsker and SR Srinivasa Varadhan. Asymptotic evaluation of certain markov process expectations for large time. iv. *Communications on Pure and Applied Mathematics*, 36(2):183–212, 1983. [5](#)
- [16] Vincent Dumoulin, Ishmael Belghazi, Ben Poole, Olivier Mastropietro, Alex Lamb, Martin Arjovsky, and Aaron Courville. Adversarially learned inference. *arXiv preprint arXiv:1606.00704*, 2016. [2](#)
- [17] Huan Fu, Mingming Gong, Chaohui Wang, Kayhan Batmanghelich, Kun Zhang, and Dacheng Tao. Geometry-consistent generative adversarial networks for one-sided unsupervised domain mapping. In *Proceedings of the IEEE Conference on Computer Vision and Pattern Recognition*, pages 2427–2436, 2019. [2](#), [3](#), [5](#), [7](#)
- [18] Leon A Gatys, Alexander S Ecker, and Matthias Bethge. Image style transfer using convolutional neural networks. In *Proceedings of the IEEE conference on computer vision and pattern recognition*, pages 2414–2423, 2016. [1](#)
- [19] Ian Goodfellow. Nips 2016 tutorial: Generative adversarial networks. *arXiv preprint arXiv:1701.00160*, 2016. [1](#)
- [20] Ian Goodfellow, Jean Pouget-Abadie, Mehdi Mirza, Bing Xu, David Warde-Farley, Sherjil Ozair, Aaron Courville, and Yoshua Bengio. Generative adversarial nets. In *Advances in neural information processing systems*, pages 2672–2680, 2014. [1](#), [2](#), [6](#)
- [21] Ishaan Gulrajani, Faruk Ahmed, Martin Arjovsky, Vincent Dumoulin, and Aaron C Courville. Improved training of wasserstein gans. In *Advances in neural information processing systems*, pages 5767–5777, 2017. [2](#)
- [22] Martin Heusel, Hubert Ramsauer, Thomas Unterthiner, Bernhard Nessler, and Sepp Hochreiter. Gans trained by a two time-scale update rule converge to a local nash equilibrium. In *Advances in neural information processing systems*, pages 6626–6637, 2017. [5](#)
- [23] R Devon Hjelm, Alex Fedorov, Samuel Lavoie-Marchildon, Karan Grewal, Phil Bachman, Adam Trischler, and Yoshua Bengio. Learning deep representations by mutual information estimation and maximization. *arXiv preprint arXiv:1808.06670*, 2018. [6](#), [12](#)
- [24] Xun Huang, Ming-Yu Liu, Serge Belongie, and Jan Kautz. Multimodal unsupervised image-to-image translation. In *Proceedings of the European Conference on Computer Vision (ECCV)*, pages 172–189, 2018. [1](#), [2](#), [3](#), [5](#), [7](#)
- [25] Phillip Isola, Jun-Yan Zhu, Tinghui Zhou, and Alexei A Efros. Image-to-image translation with conditional adversarial networks. In *Proceedings of the IEEE conference on computer vision and pattern recognition*, pages 1125–1134, 2017. [1](#), [2](#), [3](#), [4](#), [5](#), [6](#)
- [26] Tero Karras, Timo Aila, Samuli Laine, and Jaakko Lehtinen. Progressive growing of gans for improved quality, stability, and variation. *arXiv preprint arXiv:1710.10196*, 2017. [2](#)
- [27] Tero Karras, Samuli Laine, and Timo Aila. A style-based generator architecture for generative adversarial networks. In *Proceedings of the IEEE conference on computer vision and pattern recognition*, pages 4401–4410, 2019. [2](#)
- [28] Taeksoo Kim, Moonsu Cha, Hyunsoo Kim, Jung Kwon Lee, and Jiwon Kim. Learning to discover cross-domain relations with generative adversarial networks. *arXiv preprint arXiv:1703.05192*, 2017. [3](#)

- [29] Justin B Kinney and Gurinder S Atwal. Equitability, mutual information, and the maximal information coefficient. *Proceedings of the National Academy of Sciences*, 111(9):3354–3359, 2014. [3](#)
- [30] Anders Boesen Lindbo Larsen, Søren Kaae Sønderby, Hugo Larochelle, and Ole Winther. Autoencoding beyond pixels using a learned similarity metric. In *International conference on machine learning*, pages 1558–1566, 2016. [2](#)
- [31] Gustav Larsson, Michael Maire, and Gregory Shakhnarovich. Learning representations for automatic colorization. In *European conference on computer vision*, pages 577–593. Springer, 2016. [1](#)
- [32] Christian Ledig, Lucas Theis, Ferenc Huszár, Jose Caballero, Andrew Cunningham, Alejandro Acosta, Andrew Aitken, Alykhan Tejani, Johannes Totz, Zehan Wang, et al. Photo-realistic single image super-resolution using a generative adversarial network. In *Proceedings of the IEEE conference on computer vision and pattern recognition*, pages 4681–4690, 2017. [1](#)
- [33] Hsin-Ying Lee, Hung-Yu Tseng, Jia-Bin Huang, Maneesh Singh, and Ming-Hsuan Yang. Diverse image-to-image translation via disentangled representations. In *Proceedings of the European conference on computer vision (ECCV)*, pages 35–51, 2018. [1](#), [2](#), [3](#), [5](#), [7](#)
- [34] Hsin-Ying Lee, Hung-Yu Tseng, Qi Mao, Jia-Bin Huang, Yu-Ding Lu, Maneesh Singh, and Ming-Hsuan Yang. Drit++: Diverse image-to-image translation via disentangled representations. *International Journal of Computer Vision*, pages 1–16, 2020. [2](#), [3](#), [5](#), [7](#)
- [35] Chunyuan Li, Hao Liu, Changyou Chen, Yunchen Pu, Liqun Chen, Ricardo Henao, and Lawrence Carin. Alice: Towards understanding adversarial learning for joint distribution matching. *arXiv preprint arXiv:1709.01215*, 2017. [3](#)
- [36] Ralph Linsker. Self-organization in a perceptual network. *Computer*, 21(3):105–117, 1988. [3](#)
- [37] Ming-Yu Liu, Thomas Breuel, and Jan Kautz. Unsupervised image-to-image translation networks. In *Advances in neural information processing systems*, pages 700–708, 2017. [1](#)
- [38] Qi Mao, Hsin-Ying Lee, Hung-Yu Tseng, Siwei Ma, and Ming-Hsuan Yang. Mode seeking generative adversarial networks for diverse image synthesis. In *Proceedings of the IEEE Conference on Computer Vision and Pattern Recognition*, pages 1429–1437, 2019. [1](#), [2](#), [3](#), [4](#), [5](#), [6](#), [7](#), [12](#), [13](#)
- [39] Xudong Mao, Qing Li, Haoran Xie, Raymond YK Lau, Zhen Wang, and Stephen Paul Smolley. Least squares generative adversarial networks. In *Proceedings of the IEEE international conference on computer vision*, pages 2794–2802, 2017. [2](#)
- [40] Michael Mathieu, Camille Couprie, and Yann LeCun. Deep multi-scale video prediction beyond mean square error. *arXiv preprint arXiv:1511.05440*, 2015. [1](#), [4](#)
- [41] Mehdi Mirza and Simon Osindero. Conditional generative adversarial nets. *arXiv preprint arXiv:1411.1784*, 2014. [1](#)
- [42] Takeru Miyato, Toshiki Kataoka, Masanori Koyama, and Yuichi Yoshida. Spectral normalization for generative adversarial networks. *arXiv preprint arXiv:1802.05957*, 2018. [2](#)
- [43] XuanLong Nguyen, Martin J Wainwright, and Michael I Jordan. Estimating divergence functionals and the likelihood ratio by convex risk minimization. *IEEE Transactions on Information Theory*, 56(11):5847–5861, 2010. [5](#)
- [44] Sebastian Nowozin, Botond Cseke, and Ryota Tomioka. f-gan: Training generative neural samplers using variational divergence minimization. In *Advances in neural information processing systems*, pages 271–279, 2016. [5](#)
- [45] Aaron van den Oord, Yazhe Li, and Oriol Vinyals. Representation learning with contrastive predictive coding. *arXiv preprint arXiv:1807.03748*, 2018. [3](#)
- [46] Taesung Park, Alexei A Efros, Richard Zhang, and Jun-Yan Zhu. Contrastive learning for unpaired image-to-image translation. *arXiv preprint arXiv:2007.15651*, 2020. [3](#), [7](#)
- [47] Deepak Pathak, Philipp Krahenbuhl, Jeff Donahue, Trevor Darrell, and Alexei A Efros. Context encoders: Feature learning by inpainting. In *Proceedings of the IEEE conference on computer vision and pattern recognition*, pages 2536–2544, 2016. [1](#)
- [48] Alec Radford, Luke Metz, and Soumith Chintala. Unsupervised representation learning with deep convolutional generative adversarial networks. *arXiv preprint arXiv:1511.06434*, 2015. [2](#)
- [49] Eitan Richardson and Yair Weiss. On gans and gmms. In *Advances in Neural Information Processing Systems*, pages 5847–5858, 2018. [5](#), [12](#)
- [50] Tim Salimans, Ian Goodfellow, Wojciech Zaremba, Vicki Cheung, Alec Radford, and Xi Chen. Improved techniques for training gans. In *Advances in neural information processing systems*, pages 2234–2242, 2016. [1](#)
- [51] Akash Srivastava, Lazar Valkov, Chris Russell, Michael U Gutmann, and Charles Sutton. Veegan: Reducing mode collapse in gans using implicit variational learning. In *Advances in Neural Information Processing Systems*, pages 3308–3318, 2017. [2](#)
- [52] Christian Szegedy, Wei Liu, Yangqing Jia, Pierre Sermanet, Scott Reed, Dragomir Anguelov, Dumitru Erhan, Vincent Vanhoucke, and Andrew Rabinovich. Going deeper with convolutions. In *Proceedings of the IEEE conference on computer vision and pattern recognition*, pages 1–9, 2015. [5](#)
- [53] Dmitry Ulyanov, Andrea Vedaldi, and Victor Lempitsky. It takes (only) two: Adversarial generator-encoder networks. In *Thirty-Second AAAI Conference on Artificial Intelligence*, 2018. [2](#)
- [54] Ting-Chun Wang, Ming-Yu Liu, Jun-Yan Zhu, Andrew Tao, Jan Kautz, and Bryan Catanzaro. High-resolution image synthesis and semantic manipulation with conditional gans. In *Proceedings of the IEEE conference on computer vision and pattern recognition*, pages 8798–8807, 2018. [1](#)
- [55] Yaxing Wang, Abel Gonzalez-Garcia, Joost van de Weijer, and Luis Herranz. Sdit: Scalable and diverse cross-domain image translation. In *Proceedings of the 27th ACM International Conference on Multimedia*, pages 1267–1276, 2019. [2](#)
- [56] Dingdong Yang, Seunghoon Hong, Yunseok Jang, Tianchen Zhao, and Honglak Lee. Diversity-sensitive condi-

- tional generative adversarial networks. *arXiv preprint arXiv:1901.09024*, 2019. [2](#)
- [57] Zili Yi, Hao Zhang, Ping Tan, and Minglun Gong. Dualgan: Unsupervised dual learning for image-to-image translation. In *Proceedings of the IEEE international conference on computer vision*, pages 2849–2857, 2017. [3](#)
- [58] Xiaoming Yu, Yuanqi Chen, Shan Liu, Thomas Li, and Ge Li. Multi-mapping image-to-image translation via learning disentanglement. In *Advances in Neural Information Processing Systems*, pages 2994–3004, 2019. [2](#)
- [59] Han Zhang, Ian Goodfellow, Dimitris Metaxas, and Augustus Odena. Self-attention generative adversarial networks. In *International Conference on Machine Learning*, pages 7354–7363, 2019. [2](#)
- [60] Han Zhang, Tao Xu, Hongsheng Li, Shaoting Zhang, Xiaogang Wang, Xiaolei Huang, and Dimitris N Metaxas. Stackgan: Text to photo-realistic image synthesis with stacked generative adversarial networks. In *Proceedings of the IEEE international conference on computer vision*, pages 5907–5915, 2017. [1](#)
- [61] Richard Zhang, Phillip Isola, Alexei A Efros, Eli Shechtman, and Oliver Wang. The unreasonable effectiveness of deep features as a perceptual metric. In *Proceedings of the IEEE conference on computer vision and pattern recognition*, pages 586–595, 2018. [5](#), [6](#)
- [62] Junbo Zhao, Michael Mathieu, and Yann LeCun. Energy-based generative adversarial network. *arXiv preprint arXiv:1609.03126*, 2016. [2](#)
- [63] Lei Zhao, Qihang Mo, Sihuan Lin, Zhizhong Wang, Zhiwen Zuo, Haibo Chen, Wei Xing, and Dongming Lu. Uctgan: Diverse image inpainting based on unsupervised cross-space translation. In *Proceedings of the IEEE/CVF Conference on Computer Vision and Pattern Recognition*, pages 5741–5750, 2020. [1](#), [2](#)
- [64] Jun-Yan Zhu, Taesung Park, Phillip Isola, and Alexei A Efros. Unpaired image-to-image translation using cycle-consistent adversarial networks. In *Proceedings of the IEEE international conference on computer vision*, pages 2223–2232, 2017. [1](#), [3](#), [5](#)
- [65] Jun-Yan Zhu, Richard Zhang, Deepak Pathak, Trevor Darrell, Alexei A Efros, Oliver Wang, and Eli Shechtman. Toward multimodal image-to-image translation. In *Advances in neural information processing systems*, pages 465–476, 2017. [1](#), [2](#), [3](#), [4](#), [5](#), [6](#), [7](#), [12](#)

A. On the Latent Code Reconstruction Loss and the Variational Mutual Information Maximization

We show that the latent code reconstruction loss is closely related to the variational mutual information maximization [3, 9]. The latent code reconstruction loss is defined as follows:

$$\mathcal{L}_R = \mathbb{E}_z [\|E(G(\cdot, z)) - z\|_1] \quad (8)$$

where z is the latent code, $\hat{b} = G(\cdot, z)$ is the generated image, and $G(\cdot, z)$ and $E(\cdot)$ are the generator's and the encoder's function respectively.

From [9], the variational lower bound on the mutual information between the latent code Z and the output image \hat{B} can be derived below:

$$\begin{aligned} \mathcal{I}(Z; \hat{B}) &= H(Z) - H(Z|\hat{B}) \\ &= \mathbb{E}_{\hat{b} \sim G(\cdot, z)} [\mathbb{E}_{z \sim p(z|\hat{b})} [\log p(z|\hat{b})]] + H(Z) \\ &= \mathbb{E}_{\hat{b} \sim G(\cdot, z)} [\underbrace{D_{\text{KL}}[p(z|\hat{b}) \| q(z|\hat{b})]}_{\geq 0} + \mathbb{E}_{z \sim p(z|\hat{b})} [\log q(z|\hat{b})]] + H(Z) \\ &\geq \underbrace{\mathbb{E}_{\hat{b} \sim G(\cdot, z), z \sim p(z|\hat{b})} [\log q(z|\hat{b})]}_{\text{latent code reconstruction loss}} + H(Z) \end{aligned} \quad (9)$$

where $p(z|\hat{b})$ and $q(z|\hat{b})$ are the true posterior distribution and the variational posterior distribution respectively. If we choose the variational distribution $q(z|\hat{b})$ as a Laplace parameterized by the encoder, then we have the latent code reconstruction loss as shown in Equation 8.

B. On the Jensen-Shannon Divergence and Mutual Information

Although it has been pointed in [23], for self-containment of the paper, we also show the relation between the Jensen-Shannon Divergence (JSD) between the joint and the product of marginals and the Mutual Information (MI). They are related by Pointwise Mutual Information (PMI)

$$\text{PMI}(x; y) \equiv \log \frac{p(x, y)}{p(x)p(y)} = \log \frac{p(y|x)}{p(y)} \quad (10)$$

$$\begin{aligned} \text{MI} \equiv \mathcal{I}(X; Y) &= D_{\text{KL}} [p(x, y) \| p(x)p(y)] \\ &= \mathbb{E}_{p(x, y)} \left[\log \frac{p(x, y)}{p(x)p(y)} \right] \\ &= \mathbb{E}_{p(x, y)} [\text{PMI}(x; y)] \end{aligned} \quad (11)$$

Derivation from [23], we have

$$\begin{aligned} \text{JSD} [p(x, y) \| p(x)p(y)] &\propto \\ \mathbb{E}_{p(x, y)} \left[\log \frac{p(y|x)}{p(y)} - \left(1 + \frac{p(y)}{p(y|x)} \right) \log \left(1 + \frac{p(y|x)}{p(y)} \right) \right] \end{aligned} \quad (12)$$

The quantity inside the expectation of Equation 12 is a concave, monotonically increasing function of the ratio $\frac{p(y|x)}{p(y)}$, which is $e^{\text{PMI}(x, y)}$. Therefore, positive correlation exists between the MI and the JSD between the joint and the product of marginals.

C. Network Architecture of the Statistics Network

In this section, we show the network architecture of the statistics network. The latent code is replicated to form a feature map with $|z|$ channels and the proper spatial size to concatenate with every convolutional layer's input. The latent code is also concatenated with the last convolution layer's output to feed into the first fully-connected layer. The network architecture is shown in Table 3.

D. Sampling Strategies

We tried different sampling strategies for obtaining negative samples. A batchwise sampling strategy which takes all the non-corresponding pairs within the batch as the negative samples would easily run out of GPU memory. While the sampling strategy which obtains non-corresponding samples by resampling from one of the marginal distributions performs badly in our experiments. Instead, following [23], we exclude the positive samples from the negative samples and resample negative samples with the same size as the positive samples by generating another batch of images and sample non-corresponding latent codes for them. We find such a sampling strategy is stable and memory-efficient in our experiments.

E. Evaluation Details

For the FID, similar to [38], we randomly generate 50 images per input image in the test set. We randomly choose 100 input images and their corresponding generated images to form 5,000 generated samples. We use the 5,000 generated samples and all samples in training set to compute FID.

For the LPIPS distance, we follow the settings from [65]. We use 100 input images from the test set and sample 19 pairs of translated images for each input image. Then we average over them.

For NDB and JSD, we follow the suggestion of [49] and make sure there are at least 10 training samples for each

cluster. And similar to [38], we employ all the training samples for clustering and choose $K = 20$ bins for the Facades dataset, and $K = 50$ for other datasets.

F. More Qualitative Results under a Paired Setting

Here we display more qualitative results of our method on the Facades and the Maps datasets under a paired image-to-image translation setting in Figure 8 and Figure 9 respectively. All the translated samples are produced by synchronized latent codes on different input images.

G. More Qualitative Results under an Unpaired Setting

More qualitative results of our method on the Yosemite winter→summer and the cat→dog datasets under an unpaired setting are shown in Figure 10 and Figure 11 respectively. All the translated samples are produced by synchronized latent codes on different input images.

Statistics network			
Input image $a \in \mathbb{R}^{256 \times 256 \times 3}$ & Latent code $z \in \mathbb{R}^8$			
layer	input size	output size	non-linearity
4×4 conv. stride 2.	3+8.	32.	ELU.
4×4 conv. stride 2.	32+8.	64.	ELU.
4×4 conv. stride 2.	64+8.	128.	ELU.
4×4 conv. stride 2.	128+8.	256.	ELU.
4×4 conv. stride 2.	256+8.	512.	ELU.
4×4 conv. stride 2.	512+8.	512.	ELU.
FC.	$4 \times 4 \times 512 + 8.$	512.	ELU.
FC.	512.	1.	none.

Table 3. The statistics network’s architecture.



Figure 8. More qualitative results of our method on the Facades dataset under a paired setting.



Figure 9. More qualitative results of our method on the Maps dataset under a paired setting.

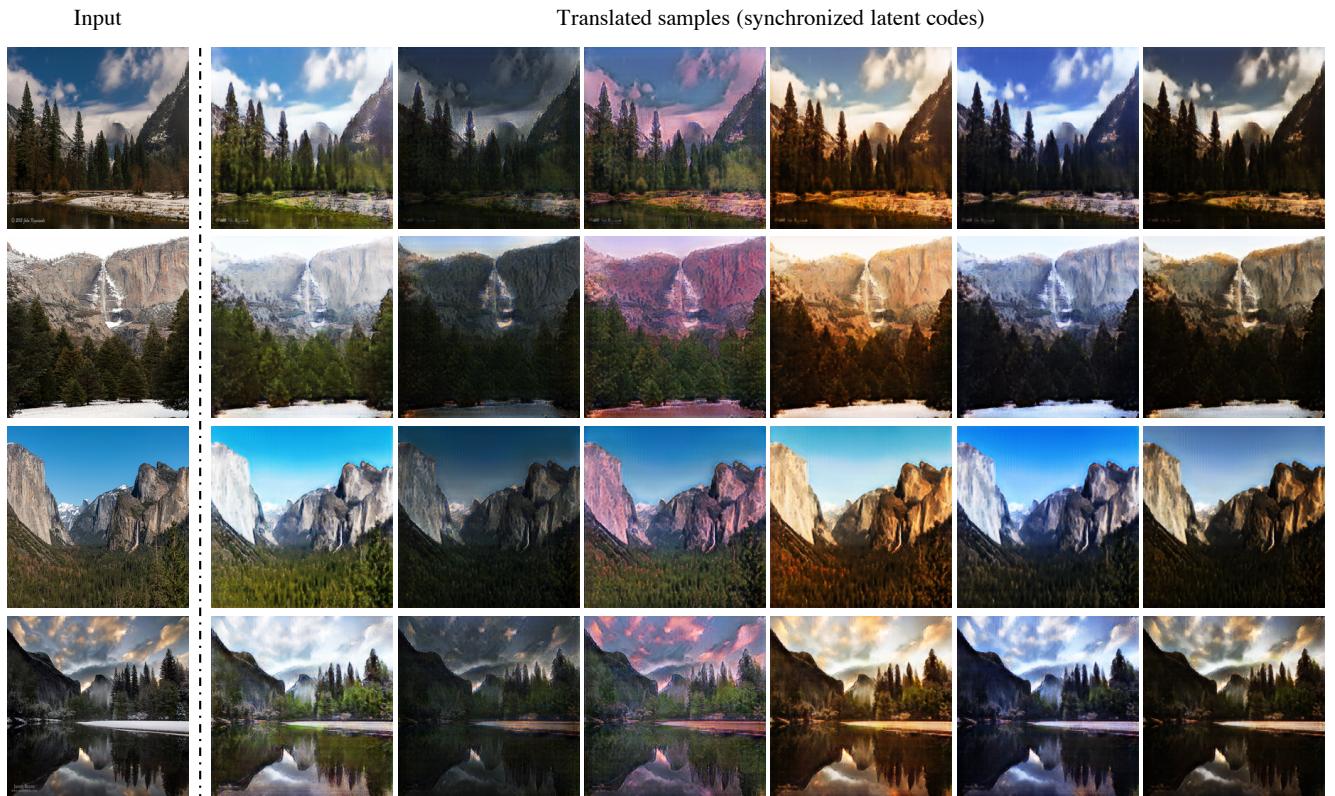


Figure 10. More qualitative results of our method on the Yosemite winter→summer dataset under an unpaired setting.

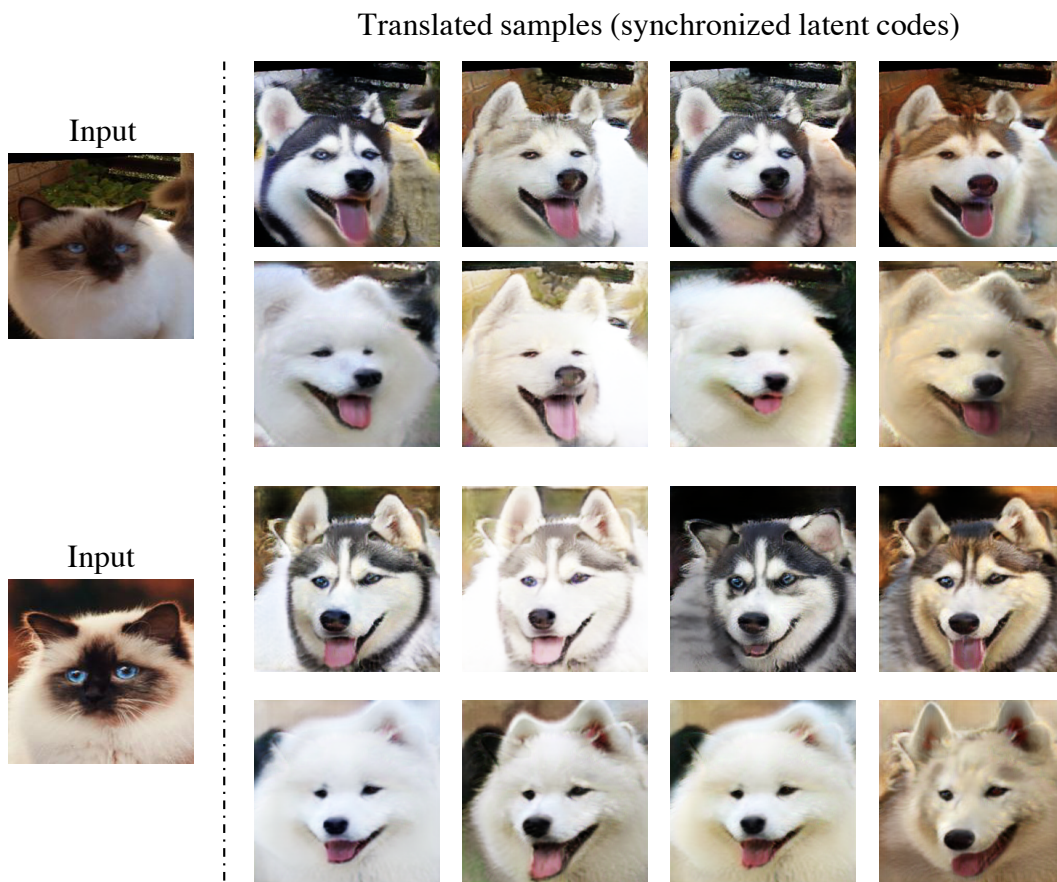


Figure 11. More qualitative results of our method on the cat→dog dataset under an unpaired setting.